Human Motion capture using Tri-Axial accelerometers

Sam Naghshineh, Golafsoun Ameri, Mazdak Zereshki
&
Dr. S. Krishnan, Dr. M. Abdoli-Eramaki

Table of Contents

3-D Virtual Real Time Upper Body Link Segment Modeling

Abstract

The purpose of this project was to design and build a low cost device to emulate upper body motion in a virtual 3D environment. Tracking human motion attracts significant attention from several areas such as animation production, ergonomics, sport medicine, and biomedical analysis. First, it was intended to detect human motion by using accelerometers. However, after conducting many research and experiments, it was concluded that accelerometers have limitations in detecting motion. In other words, one accelerometer alone cannot detect horizontal movements (on any horizontal ring on a sphere) when there is no dynamic acceleration. One of the proposed and tested solutions was to use compass sensors to compensate for the accelerometers limitations. Therefore, eight accelerometers were used to detect the motion of arms, head, neck, and back and four compass sensors were used to detect the horizontal movement of the back at various angles. The experiment was successfully done and satisfactory results were obtained. The other proposed method which was tested for one body segment and compared to the first solution was to use gyroscopes along with accelerometers. Even though using a gyroscope would improve the results significantly, due to the high cost of gyroscopes and time limitations this method was not implemented. However, using gyroscopes are highly recommended for future design. The 3-D virtual LSM used in this project to validate how well the system tracks motion was a courtesy of Dr. Abdoli- Eramaki's laboratory. To

1 Introduction

The study of human body segment movements attracts significant attention from several areas such as animation production, video game console, ergonomics, sport medicine, rehabilitation and biomedical analysis. This project was inspired by the Occupational Health Department at Ryerson University. “Manual material handling, particularly lifting poses a risk to many workers and is considered a major cause of work-related low-back pain and impairment. The total cost of low-back pain disorders in the United States was estimated to be $90 billion in 1998, and costs have continued to increase. The increased prevalence of low-back pain in the world and its potential future magnitude has motivated many researchers to search for the best methods for estimating the conditions that can potentially increase the incidence of back pain. Bio-mechanical models such as Link Segment Model (LSM) are used for calculation of forces and moments on all human joints since direct measurements of forces and moments are not practical or feasible in most cases. With the aid of these models, organizations like National Institute or Occupational Safety and Health (NIOSH), have developed equations and guidelines designed to help practitioners and engineers design workplaces that are less problematic for workers” [1].

To test the accuracy and precision of devices promising to reduce the forces and moments on human body, such as lumbar spine or lower back, there is the need to monitor body movements and analyzing the obtained data.

Medical literature can be found about the use of accelerometers in biomedical applications to study body movements. Several research groups face the problem of movement evaluation with the aim of modeling human movements and for rehabilitation or graphic representation purposes. Two widespread systems are used for the evaluation of human body movements which are depicted as follows. The ELITE project is an electronic system dating back to the 80’s. It was based on CCD cameras to catch motion pictures of the subject with artificial passive markers and able to automatically analyze 3D movements, thanks to pattern recognition algorithms implemented on parallel special purpose architecture. Another proposal is Constellation, a tracking system for interactive graphic applications which require smooth and fast free space tracking of user body, based on an inertial navigation system aided by ultrasonic time-of-flight

range measurements to a constellation of wireless transponder beacons. Constellation operates indoors, has much finer resolution and accuracy. Just as Global Positioning Systems (GPS) have a space-based constellation of satellites and a vehicle-born receiver with antennas, this system has a ceiling-based constellation of transponder beacons. The described solutions require a suitable environment for measurements. A solution to the problem could be stand-alone, portable motion capture device.

The objective of this project is to design the hardware of a wireless stand-alone 3D human body motion detector as well as to implement the software for real time tracking of 8 of these sensors in a virtual environment. Next to the problem of human motion emulation, other issues such as the weight of the system, the power supply, and the destructive interference with electromagnetic fields or ferromagnetic materials were considered when designing a stand-alone posture and body movement detector. This device helps the researchers be able to calculate the force on the lower back and lumbar spine on a body instantaneously and evaluate the effectiveness of devices that help reduce the force on the lower back.

2 Theory

In this section, detailed explanations on the theory behind the main concepts that directly influenced the design of the 3D Real Time Human Body Motion Detector are provided. Such main concepts are: Calculating angles and rotations using accelerometers, compass sensor, gyroscope, Euler angles, gimbal lock, quaternions, conversion between Euler angles to Quaternion, SPI, real time computing, and different approaches that were taken to find angles.

2.1 Calculating angles and rotations using accelerometers

In this section a brief introduction to accelerometers are provided as well as different ways of tilt sensing and angle measurement using accelerometers.

2.1.1 Accelerometer

An accelerometer is a device that converts acceleration into an electrical signal. Both dynamic and static acceleration can be measured using an accelerometer where dynamic acceleration is the acceleration due to any force except for the gravitational force applied on a rigid body and the static acceleration (or gravitational acceleration) is due to the gravitational force. The output of an accelerometer can be analog or digital. In the analog case, the output voltage or the duty cycle of a square wave is directly proportional to the acceleration. On the other hand, the output of a digital accelerometer can be directly accessed using protocols such as SPI. Many other parameters such as the number of axes, maximum swing, sensitivity and bandwidth define different accelerometers for a variety of practical purposes. Three of the most important techniques to measure acceleration are explained briefly below.

- Piezoelectric Accelerometer

  This kind of accelerometers makes use of the piezoelectric effect. As the piezo-element is compressed due to force caused by acceleration, or subject to a shearing force, a proportional electrical signal is generated. Piezoelectric accelerometers are not suitable for measuring zero acceleration conditions (DC), but are well suited for high frequency vibrations.
- Capacitive Accelerometer

This kind of accelerometer is similar to the piezoelectric accelerometer except that it uses capacitive effect. Since this kind of accelerometers can be micro-machined in silicon, they can be used in integrated circuits.

- Thermal Accelerometer

  Inside a thermal accelerometer there is a heater to heat up a small bubble of air inside of the IC. The position of the heated air bubble is changed as force is applied on to the accelerometer. The movement of the heated bubble is measured by temperature sensors and then converted to an electrical signal.

2.1.2 Dual-Axis and Tri-Axis Tilt sensing

- Dual-Axis Tilt Sensing

Low-g dual–axis (X,Y) accelerometers are often used in angle/tilt sensing applications where the force of gravity is used as an input to determine the orientation of an object. The sensor is most responsive to changes in tilt when the sensitive axis is perpendicular to the force of gravity and is least responsive to changes in tilt when the sensitive axis is oriented in +g or –g position. When horizontally mounted, a dual–axis accelerometer's diminishing sensitivity through increased tilt prevents accurate angle/tilt measurement when the accelerometer is tilted beyond 45° along either axis. Also the absence of a Z-axis sensor indicates that the accelerometer cannot detect an inversion, causing improper functioning.

- Tri-Axis Tilt Sensing

In tri-axial accelerometers, X, Y, and Z axes can sense tilt. The Z axis can be combined with both of the tilting axes to improve angle/tilt sense precision and accuracy. As shown in figure 1the X and Y axis follow the sine function while the Z axis follows the cosine function.

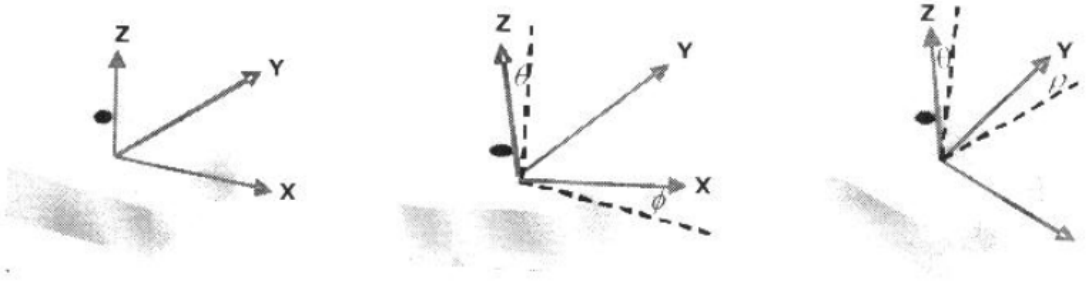

Figure 1 : X, Y and Z axes tilt relative to ground

Therefore, if φ and ρ represent the angles that the X and Y accelerometer maxes make with the fixed reference XY plane, and Θ is the angle of the Z axis relative to gravity, these angles can be calculated as the following.

$$\varphi = \arcsin(a_x)$$

$$\rho = \arcsin(a_y)$$

$$\Theta = \arccos(a_z)$$

To maintain better and constant sensitivity through all 360° of tilt, the Z axis can be combined with the X and/or Y axes. In the following subsections, angle measurement using one, two , and three axes are explained in more detail.

2.1.3 Angle Measurement

Tilt is a static measurement. The force of gravity is used as an input to determine the orientation of an object calculating the degree of tilt. Some accelerometers can sense up to 3g. However, to simplify the concept of tilt measurement, the following angle measurement methods are based on accelerometers sensing acceleration in the range of -1g to 1g through 180° of tilt. In general, the accuracy of the tilt measurement can be improved by implementing a 0g calibration routine for the accelerometer to compensate for the 0g offset. To understand how to acquire a reliable and accurate tilt reading from accelerometers, various techniques on measuring tilt are explained in detail here.

- Measuring tilt using one axis

  In the case of a dual-axis accelerometer (XY) mounted perpendicular to gravity the tilt algorithm is limited to one axis of sensitivity. As shown in figure 2 the accelerometer is tilted along the x-axis. The Y-axis remains at 0g output throughout the full rotation of the X-axis in this case.

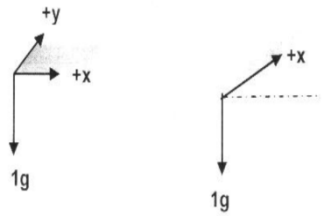

Figure 3: Dual-axis accelerometer with one axis of tilt

If one axis (X-axis) is used to calculate the tilted angle of the accelerometer the following trigonometric relationship is used:

$$V_{outx} = V_{off} + S(\sin\Theta)$$

Where V_{outx} is the output voltage from the X-axis of the accelerometer, V_{off} is the offset voltage, and S is the sensitivity of the accelerometer. The acceleration output on the X-axis due to the gravity is:

$$A_x = \frac{Voutx - Voff}{S}$$

Therefore, the angle of tilt becomes the following:

$$\Theta = \sin^{-1}(A_x)$$

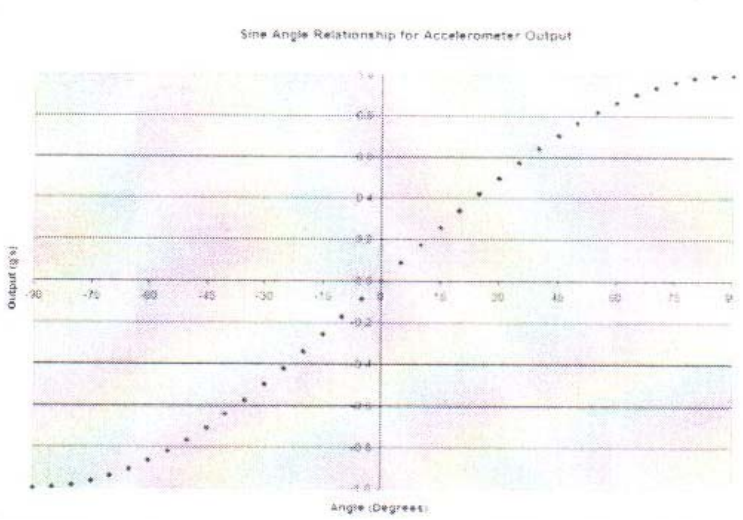

Figure 4: Accelerometer's output when tilted from -90° to 90°

The graph shows that the output in g's of the accelerometer as it tilts from -90° to +90°. The sensitivity diminishes between -90° and -45° and between +45° to +90°. This resolution problem makes this method of calculating the angle of tilt inaccurate when the accelerometer's output is near +1g or -1g. Another disadvantage of the single axis tilt measurement technique is that it is impossible to know the difference between two tilt angles that result in the same sensor output. Since the output is a sine function, it could not be concluded from the accelerometer output (Θ°) that the amount of tilt was Θ° or 180°-Θ°. As a result, one would have to be aware of the correct orientation of the accelerometer and have a sense for the quadrant of tilt. The disadvantages of this technique can be overcome by using a two axis measurement tilt technique.

- Measuring tilt using two axes

  The resolution problems and tilt orientation difficulties can be addressed by mounting the accelerometer vertically so that the y-axis is parallel to gravity, or by using tri-axis accelerometer using at least 2 or 3 axis. Using more than one axis to calculate tilt produces a more accurate solution.

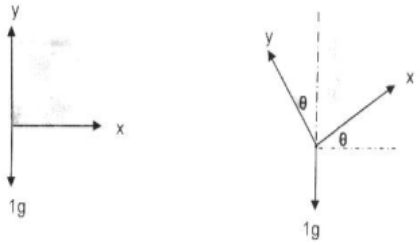

Figure 5: Using a dual or tri-axis accelerometer with two axes for measuring tilt

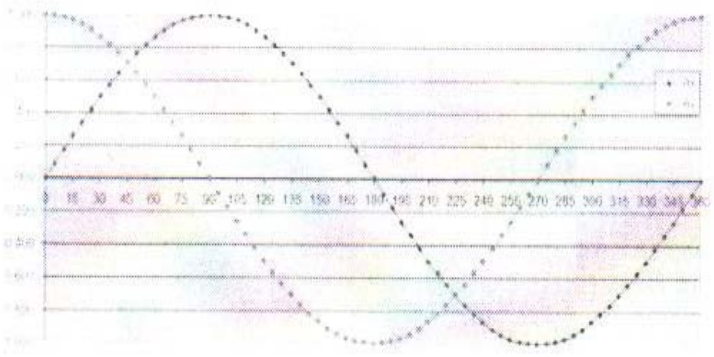

Figure 6: Sine function of the X output and Cosine function of the Y output

The graph above shows that when using a two axis solution the component due to gravity on the X-axis follows the sine function while the component due to gravity acting on the Y-axis follows the cosine function. It is observed that the sensitivity (slope of the line) in the X direction is at its maximum while the Y sensitivity is at its minimum and vise versa. Therefore, maximum tilt sensitivity can be maintained if both the X and Y outputs are combined. Considering the simple trigonometry shown below based on figure 5, Θ can be found by combining A_x and A_y.

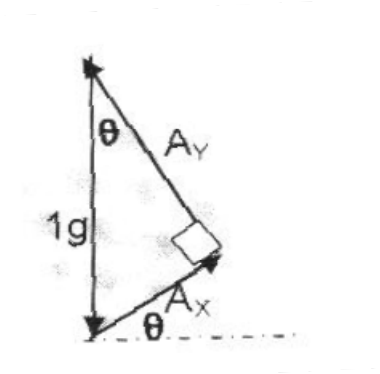

Figure 7: basic trigonometry of sensed accelerations

$A_x = \sin\Theta$

$A_y = \cos\Theta$

$A_x / A_y = \tan\Theta \rightarrow \Theta = \arctan (A_x / A_y)$

It is important to note that the combined acceleration is always 1g:

$A = \sqrt{(A^2_x + A^2_y)} = 1g$

The sensor is most sensitive to changes in tilt when the sensitive axis is perpendicular to the force of gravity and is least sensitive when the sensitive axis is parallel to the force of gravity in the +1g or -1g. This is illustrated in figure 8 where the absolute value of the tilt sensitivity was taken. As the X-axis is at its minimum tilt sensitivity the Y-axis was at its maximum tilt sensitivity.

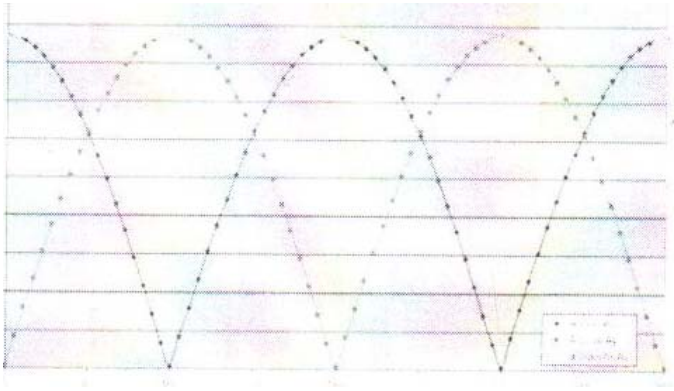

Figure 8: Tilt sensitivity versus tilt angle

It is important to know the X and Y accelerations to determine the quadrant of tilt that is applicable because the output from the first and third quadrant will also be the same. For example, tan(45) =1 and tan(225) =1. When taking the arctan of a positive value the tilt angle is in either the first or the third quadrant. Knowing the sign of A_x and A_y will

determine exactly which quadrant. When taking the arctan of a negative value, the tilt angle is in either the second or the forth quadrant. Knowing the sign if A_x and A_y will determine quadrant the accelerometer is tilting through. Therefore,

If in quadrant 1 = $\arctan(A_x/ A_y)$

If in quadrant 2 = $\arctan(A_x/ A_y) + 180$

If in quadrant 3 = $\arctan(A_x/ A_y) + 180$

If in quadrant 4 = $\arctan(A_x/ A_y) + 360$

- Measuring tilt using three axis

  In order to define the angles of the accelerometer in three dimensions, the pitch, roll and theta are sensed using all three outputs of the acceleration. Pitch (ρ) is defined as the angle of X-axis relative to ground. Roll (φ) is defined as the angle of the Y-axis relative to ground, and theta (Θ) is the angle of the Z-axis relative to gravity.

  $\rho = \arctan(A_x/ \sqrt{(A^2_Y + A^2_Z)})$

  $\varphi = \arctan(A_Y/ \sqrt{(A^2_X + A^2_Z)})$

  $\Theta = \arctan((\sqrt{(A^2_X + A^2_Y)})/A_Z)$

  Now, the acceleration due to gravity on the X-axis, Y-axis and Z-axis are combined. The resultant sum of the accelerations from the three axes is equal to 1g when the acceleration is static.

$$\sqrt{(A^2_X + A^2_Y + A^2_Z)} = 1g$$

2.2 Compass Sensor

Compass sensor is a dual-axis magnetic field sensor which when hold horizontally can detect the magnetic field of the Earth. The compass that was used in this project has two axes, x and y. Each axis reports the strength of the magnetic field's component parallel to it. The x-axis reports (field strength) × cos(θ), and the y-axis reports the (field strength) × sin(θ). To resolve θ into a clockwise angle from north, use arctan(-y/x). This device would return a value of 1 for a north magnetic field of 1 μT parallel to one of its axes. If the magnetic field is south, the value will be -1.

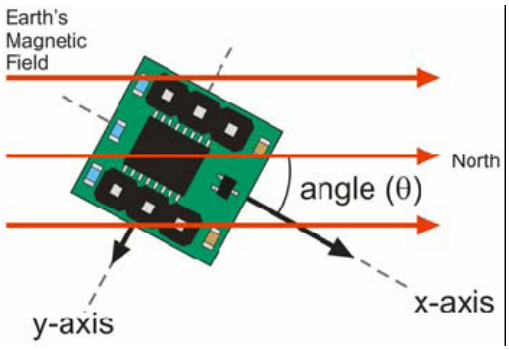

Figure 9: The compass sensor

2.3 Gyroscope

Gyroscopes are used to measure angular rate which is how quickly an object turns. The rotation is typically measured in reference to one of three axes: yaw, pitch, or roll. Depending on how a gyroscope normally sits, its primary axis of sensitivity can be one of the three axes of motion: yaw, pitch, or roll. A gyroscope with one axis of sensitivity can also be used to measure other axes by mounting the gyroscope differently. As an example of how a gyroscope could be used, a yaw-axis gyroscope mounted on a turntable rotating at 33 1/3 rpm (revolutions per minute) would measure a constant rotation of 360 ° times 33 1/3 rpm divided by 60 seconds, or 200 ° /seconds. The gyroscope would output a voltage proportional to the angular rate, as determined by its sensitivity, measured in mille Volts per degree per second (mV/ ° /s). The full-scale voltage determines how much angular rate can be measured, so in the example of the turntable, a gyroscope would need to have a full scale voltage corresponding to at least 200 ° /seconds. Full-scale is limited by the available voltage swing divided by the sensitivity. Most gyroscopes measure angular rate by means of Coriolis acceleration. The Coriolis effect can be explained as follows. Consider yourself standing on a rotating platform, near the center. If you were to move to a point near the outer edge of the platform, your speed would increase relative to the ground, as indicated by the longer arrow. The rate of increase of the tangential speed, caused by the radial velocity, is the *Coriolis* acceleration (after Gaspard G. de Coriolis, 1792–1843—a French mathematician). If Ω is the angular rate and r the radius, the tangential velocity is Ω r. So, if r changes at speed, v, there will be a tangential acceleration Ω v. This is half of the Coriolis acceleration. There is another half from changing the direction of the radial velocity giving a total of 2 Ω v. For mass M, the platform must apply a force, 2 M Ω v, to cause that acceleration,

and the mass experiences a corresponding reaction force. One of the most important concerns for a gyroscope user is the device' s ability to reliably provide an accurate angular-rate output signal even in the presence of environmental shock and vibration.

2.4 Euler Angles

Euler angles, first developed by Leonhard Euler, are defined as a means of representing the spatial orientation of any frame of the space as a composition of rotations from a reference frame. The Euler angles describe the orientation of a rigid body (in which the relative position of all its points is constant) in 3-dimensional Euclidean space. The orientation of a body in 3-dimensional space can be specified by decomposing its three rotations described by Euler angels with respect to a fixed coordinate system. According to Euler's rotation theorem, any rotation may be described using three angles. Figure 1 illustrates the fixed system, denoted in lower case (x,y,z), and the rotated system, denoted in upper case letters (X,Y,Z). By defining the intersection of the xy and the XY coordinate planes as the line of nodes (N), the angles shown in figure 1 are as the following.

- α is the angle between the x-axis and the line of nodes
- β is the angle between the z-axis and the Z-axis
- γ is the angle between the line of nodes and the X-axis

α and γ are defined as modulo 2 radians having a valid range of $[-\pi, \pi]$. However, the range for β is modulo radians which could be $[0, \pi]$ or $[-\pi/2, \pi/2]$.

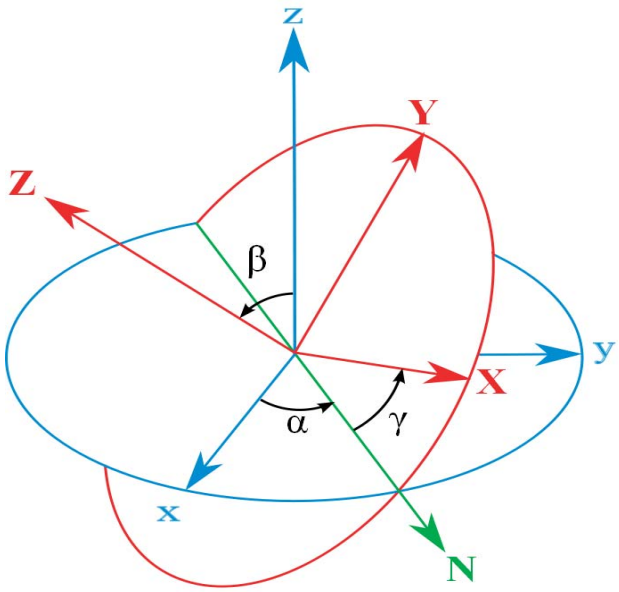

Figure 10: The xyz (fixed) system is shown in blue, the XYZ (rotated) system is shown in red [http://en.wikipedia.org/wiki/Euler_angles]

2.4.1 Euler Rotations

According to Euler's rotation theorem, any rotation may be described using three angles. Euler rotations are obtained by changing one of the Euler angles while leaving the other two constant. Euler rotations are expressed utilizing both the external frame and the co-moving rotated body frame. They constitute mixed axes of rotation system, where the first angle moves the line of nodes around the external axis z; the second angle rotates around the line of nodes and the third one is an intrinsic rotation around an axis fixed in the body that moves. One of the important characteristics of these rotations is that they are commutative which results in obtaining the same results regarding the orientation of a body regardless of the order in which they are applied.

2.4.2 Matrix Notation

In a 3-dimensional coordinate axes, called intermediate frames with their origin in common, any target can be reached by performing three simple rotations, since the two first rotations determine the new Z axis and the third rotation will obtain all the orientation possibilities that this Z axis allows. A matrix representing the end result of all three rotations representing an orientation in 3D space is formed by successive multiplication of the matrices representing the three simple rotations, as illustrated in the following transformation equation.

$$\mathbf{p}' = \mathbf{pR}$$
$$= [x, y, z] \begin{bmatrix} \cos\alpha & -\sin\alpha & 0 \\ \sin\alpha & \cos\alpha & 0 \\ 0 & 0 & 1 \end{bmatrix} \begin{bmatrix} 1 & 0 & 0 \\ 0 & \cos\beta & -\sin\beta \\ 0 & \sin\beta & \cos\beta \end{bmatrix} \begin{bmatrix} \cos\gamma & -\sin\gamma & 0 \\ \sin\gamma & \cos\gamma & 0 \\ 0 & 0 & 1 \end{bmatrix}$$

where

- The leftmost matrix represents a rotation around the axis ' z ' of the original reference frame
- The middle matrix represents a rotation around an intermediate ' x ' axis which is the "line of nodes"
- The rightmost matrix represents a rotation around the axis ' Z ' of the final reference frame

The following matrix is obtained by carrying out the matrix multiplication, and abbreviating the sine and cosine functions as s and c, respectively:

$$[\mathbf{R}] = \begin{bmatrix} \mathrm{c}_\alpha \mathrm{c}_\gamma - \mathrm{s}_\alpha \mathrm{c}_\beta \mathrm{s}_\gamma & -\mathrm{c}_\alpha \mathrm{s}_\gamma - \mathrm{s}_\alpha \mathrm{c}_\beta \mathrm{c}_\gamma & \mathrm{s}_\beta \mathrm{s}_\alpha \\ \mathrm{s}_\alpha \mathrm{c}_\gamma + \mathrm{c}_\alpha \mathrm{c}_\beta \mathrm{s}_\gamma & -\mathrm{s}_\alpha \mathrm{s}_\gamma + \mathrm{c}_\alpha \mathrm{c}_\beta \mathrm{c}_\gamma & -\mathrm{s}_\beta \mathrm{c}_\alpha \\ \mathrm{s}_\beta \mathrm{s}_\gamma & \mathrm{s}_\beta \mathrm{c}_\gamma & \mathrm{c}_\beta \end{bmatrix}.$$

2.5 Gimbal Lock

"Gimbal lock is defined as the loss of one degree of freedom which occurs when the axes of two of the three gimbals needed to apply or compensate for rotations in three dimensional space are driven to the same direction. A gimbal is a ring that is suspended so it can rotate about an axis. Gimbals are typically nested one within another to accommodate rotation about multiple axes. They appear in gyroscopes and in inertial measurement units to allow the inner gimbal's orientation to remain fixed while the outer gimbal suspension assumes any orientation, in compasses, flywheel energy storage or more commonly drink holders to allow things to remain horizontal. They are used to orientate thrusters on a rocket. Some coordinate systems in mathematics behave as if there were real gimbals used to measure the angles. For cases of at least three nested gimbals mounted in a certain way, gimbal lock can occur."

The angles α, β and γ are uniquely determined except for the singular case that the xy and the XY planes are identical, while the z axis and the Z axis having the same or opposite directions. Indeed, if the z axis and the Z axis are the same, β = 0 and only (α+ γ) is uniquely defined (not the individual values). Similarly, if the z axis and the Z axis are opposite, β = π and only (α - γ) is

uniquely defined (not the individual values). These ambiguities are known as gimbal lock in applications.

2.5.1 Loss of a degree of freedom with Euler angles

In the previous section a rotation in 3D space, based on Euler rotations, was obtained and represented as matrix R. When _ is equal to zero which is known as the singular case, matrix R will reduce to

$$\left[\ R\ \right] = \begin{bmatrix} cos\alpha cos\gamma - sin\alpha sin\gamma & -cos\alpha sin\gamma - sin\alpha cos\gamma & 0 \\ sin\alpha cos\gamma + cos\alpha sin\gamma & -sin\alpha sin\gamma + cos\alpha cos\gamma & 0 \\ 0 & 0 & 1 \end{bmatrix}$$

Therefore,

$$\left[\ R\ \right] = \begin{bmatrix} cos(\alpha+\gamma) & -sin(\alpha+\gamma) & 0 \\ sin(\alpha+\gamma) & cos(\alpha+\gamma) & 0 \\ 0 & 0 & 1 \end{bmatrix}$$

Changing α and γ 's values in the above matrix would change the rotation's angle $\alpha + \gamma$ while remaining the rotation's axis in the Z direction. The last column and the last line in the matrix won't change: one degree of freedom has been lost. The only solution for α and γ to recover different roles would be to assign a non zero value to β. A similar problem appears when $\beta = \pi$.
There would always at least one value for which a degree of freedom is lost using Euler angles even if another convention for representing a rotation with a matrix using Euler angles were employed or other variation intervals for the angles that were chosen. However, more distinct solutions than the degree of the polynomial the gumball lock problem does not make Euler angles "wrong" (they always play their role of a coordinates system); it just makes them unsuited for a number of practical applications.

2.5.2 Solution To Gimbal Lock

The best way to avoid the gumball lock is to acquire quaternions for representing rotations in 3D space. In the next section, representation of rotations using quaternions is explained in detail.

2.6 Quaternion

"Quaternions, in mathematics, are a non-commutative number system that extends the complex numbers. The quaternions were first described by the Irish mathematician Sir William Rowan Hamilton in 1843 and applied to mechanics in three-dimensional space. They find uses in both theoretical and applied mathematics, in particular for calculations involving three-dimensional

rotations, such as in 3D computer graphics, although they have been superseded in many applications by vectors and matrices. In modern language, quaternions form a 4-dimensional normed division algebra over the real numbers. The algebra of quaternions is often denoted by H (for Hamilton). As a set, the quaternions H are equal to R^4, a four-dimensional vector space over the real numbers. H has three operations: Addition, scalar multiplication, and quaternion multiplication. The sum of two elements of H is defined to be their sum as elements of R^4. Similarly the product of an element of H by a real number is defined to be the same as the product in R^4. To define multiplication in H requires a choice of basis for R^4. The elements of this basis are customarily denoted as 1, i, j, and k. Every element of H can be uniquely written as a linear combination of these basis elements, that is, as a1 + bi + cj + dk, where a, b, c, and d are real numbers. The basis element 1 will be the identity element of H, meaning that multiplication by 1 does nothing, and for this reason, elements of H are usually written as a + bi + cj + dk, suppressing the basis element 1. Given this basis, quaternion multiplication is defined by first defining the products of basis elements and then defining all other products using the distributive law." There is no problem similar to the gimbal lock with quaternions. This can be explained intuitively by the fact that a quaternion describes a rotation in one single move. More details on quaternion and spatial rotations are provided in the following sections.

2.6.1 Remarks

- Non-commutability

Unlike multiplication of real or complex numbers, multiplication of quaternions is not commutative. For example, ij = k, while ji = k. The non-commutability of multiplication has some unexpected consequences such as obtaining more distinct solutions than the degree of the polynomial when solving polynomial equations over the quaternions. "The equation z2 + 1 = 0, for instance, has infinitely many quaternion solutions z = bi + cj + dk with b2 + c2 + d2 = 1, so that these solutions form a two-dimensional sphere centered on zero in the three-dimensional pure imaginary subspace of q quaternions. This sphere intersects the complex plane at the two poles i and i."

- Quaternions and the geometry of R^3

"Because the vector part of a quaternion is a vector in R3, the geometry of R3 is reflected in the algebraic structure of the quaternions. Many operations on vectors can be defined in terms of

quaternions, and this makes it possible to apply quaternion techniques wherever spatial vectors arise. For instance, this is true in electrodynamics, general relativity, and 3D computer graphics."

2.6.2 Quaternions and spatial rotation

Unit quaternions provide a convenient mathematical notation for representing orientations and rotations of objects in three dimensions. Compared to Euler angles, unit quaternions are simpler to compose and avoid the problem of gimbal lock. Also, compared to rotation matrices, they are more numerically stable and may be more efficient. Quaternions have applications in computer graphics, robotics, navigation, Molecular Dynamics and orbital mechanics of satellites.

- Visualizing the space of rotations

"Unit quaternions represent in a very straightforward way the mathematical space of rotations in three dimensions. The correspondence between rotations and quaternions can be understood by first visualizing the space of rotations itself. Any rotation in three dimensions is a rotation by some angle about some axis. When the angle is zero the axis does not matter, so rotation by zero degrees is a single point in the space of rotations (the identity rotation). For a tiny but nonzero angle, the set of possible rotations is like a small sphere surrounding the identity rotation, where each point on the sphere represents an axis pointing in a particular direction (compare the celestial sphere). Rotations through increasingly large angles are increasingly far from the identity rotation, and we can think of them as concentric spheres of increasing radius. Thus, near the identity rotation, the abstract space of rotations looks similar to ordinary three-dimensional space (which can also be seen as a central point surrounded by concentric spheres of every radius). However, as the rotation angle increases toward 360°, rotations about different axes stop diverging and become more similar to each other, becoming identical (and equal to the identity rotation) when the angle reaches 360°. We can see similar behavior on the surface of a sphere. If we start at the North Pole and draw straight lines (that is, lines of longitude) in many directions, they will diverge but eventually converge again at the South Pole. Concentric circles of increasing radius drawn around the North Pole (lines of latitude) will eventually collapse to a point at the South Pole once the radius reaches the distance between the poles. If we think of different directions from the pole (that is, different longitudes) as different rotation axes, and different distances from the pole (that is, different latitudes) as different rotation angles, we have an analogy to the space of rotations. Since the sphere's surface is two dimensional while the space of rotations is three dimensional, we must actually model the space of rotations as a hyper-

sphere; however, we can think of the ordinary sphere as a slice through the full hyper-sphere (just as a circle is a slice through a sphere). We can take the slice to represent, for example, just the rotations about axes in the xy plane. Note that the angle of rotation is twice the latitude difference from the North Pole: points on the equator represent rotations of 180°, not 90°, and the south pole represents a rotation of 360°, not 180°.The north pole and the south pole represent the same rotation, and in fact this is true of any two antipodal points: if one is a rotation by around the axis v, the other is a rotation by 360° - α around the axis -v. In fact, then, the space of rotations is not the (hyper) sphere itself but the (hyper) sphere with antipodal points identified. But for many purposes we can think of rotations as points on the sphere, even though they are twofold redundant (a so-called double cover)."

2.6.3 Quaternion in Matrix Form

A unit quaternion can be described as:

$$q = \begin{bmatrix} q_1 & q_2 & q_3 & q_4 \end{bmatrix}^T$$
$$|q|^2 = q_1^2 + q_2^2 + q_3^2 + q_4^2 = 1$$

We can associate a quaternion with a rotation around an axis by the following expression

$$q_0 = \cos(\alpha/2)$$
$$q_1 = \sin(\alpha/2)\cos(\beta_x)$$
$$q_2 = \sin(\alpha/2)\cos(\beta_y)$$
$$q_3 = \sin(\alpha/2)\cos(\beta_z)$$

where is a simple rotation angle (the value in radians of the angle of rotation) and cos(x), cos(y) and cos(z) are the "direction cosines" locating the axis of rotation (Euler's Theorem).

2.7 Euler to Quaternion Conversion

The conversion equations are provided on the next page.

$$q_1 = cos(\frac{R}{2})cos(\frac{P}{2})cos(\frac{Y}{2}) \pm sin(\frac{R}{2})sin(\frac{P}{2})sin(Y2)$$
$$q_2 = -sin(\frac{R}{2})cos(\frac{P}{2})cos(\frac{Y}{2}) \pm cos(\frac{R}{2})sin(\frac{P}{2})sin(Y2)$$
$$q_3 = -cos(\frac{R}{2})sin(\frac{P}{2})cos(\frac{Y}{2}) \pm sin(\frac{R}{2})cos(\frac{P}{2})sin(Y2)$$
$$q_4 = -cos(\frac{R}{2})cos(\frac{P}{2})sin(\frac{Y}{2}) \pm sin(\frac{R}{2})sin(\frac{P}{2})cos(Y2)$$

Seq	RPY	RYP	PYR	PRY	YRP	YPR
q_1	-	+	-	+	-	+
q_2	-	+	-	-	+	+
q_3	+	+	-	+	-	-
q_4	-	-	+	+	-	+

2.8 SPI

"The Serial Peripheral Interface Bus or SPI bus is a synchronous serial data link standard named by Motorola that operates in full duplex mode". Devices communicate in master/slave mode where the master device initiates the data frame. Multiple slave devices are allowed with individual slave select (chip select) lines. Sometimes SPI is called a "four wire" serial bus, contrasting with three, two, and one wire serial buses. Being a synchronous interface, SPI requires the same clock signal to be used by the SPI subsystem and the external device. The SPI bus can operate with a single master device and with one or more slave devices. SPI communication is a low level communication that does not provide any of the fancier communication features such as peripheral addressing and data acknowledgement available in other protocols. All other peripherals that are not enabled should ignore the other lines by tri-stating the bus.

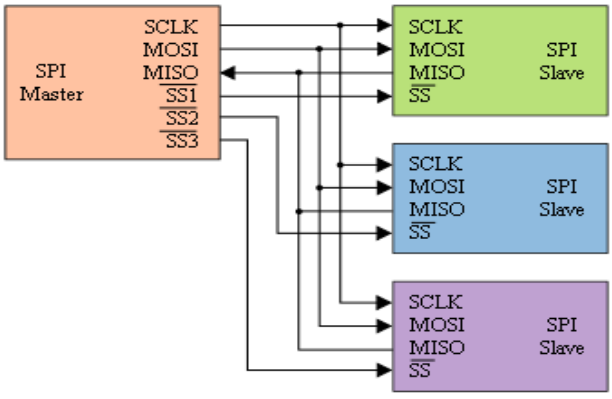

Figure 11: SPI multiple slave configuration

2.8.1 Data Transmission

To begin a communication, the master first configures the clock, using a frequency less than or equal to the maximum frequency the slave device supports. The master then pulls the slave select low for the desired chip. If a waiting period is required (such as for analog-to-digital conversion) then he master must wait for at least that period of time before starting to issue clock cycles. During each SPI clock cycle, a full duplex data transmission occurs:

- the master sends a bit on the MOSI line; the slave reads it from that same line
- the slave sends a bit on the MISO line; the master reads it from that same line

2.9 Real Time Computing

In computer science, real-time computing (RTC) is the study of hardware and software systems that are subject to a "real-time constraint" i.e. operational deadlines from event to system response.

2.10 Different Approaches Taken to Find Angles

1. Integral approach

The first approach that was thought of for tracking human motion using accelerometers was to measure the acceleration during body movement and then find the displacement by taking the second integral of the measured acceleration. The LSM could be then modified to take the displacement as input to display the movement. One of the problems with this method was that the length of the arm of the person using the device needed to be measured and considered in calculations. Therefore, the device would practically introduce some limitations since it would be dependent on getting specific information from the user. Another problem with this approach was that the accuracy of the device would decrease drastically when it was used for a long time. The reason is that electrical instruments such as accelerometers have limited accuracy. Therefore, there would be some deviation from the actual distance made during body motion with the calculated distance using the accelerometer. Moreover, the calculated distance for each motion would be based on the detected distance of the previous motion (used as a reference point). Therefore, if there is some error in the first calculated distance, the second calculated distance will have more error since the error caused by the accelerometer would be added to the error in calculating previous distance. In other words, the error would be accumulated and the system would not perform well after a short while.

2. Global measurement

In the Global approach, angles of each axis in any octant with respect to the gravitational force were calculated. However, it was observed that the obtained values of angles for each 2 octants would be the same. This phenomenon was the result of lacking one degree of freedom. As shown below, it is not possible to find three angles in the range of 0° to 360°. However, one can find angles in the range of -90° to 90° by using one accelerometer. Since the axes of accelerometer are perpendicular to each other, the movement of one axis depends on the other two axes.

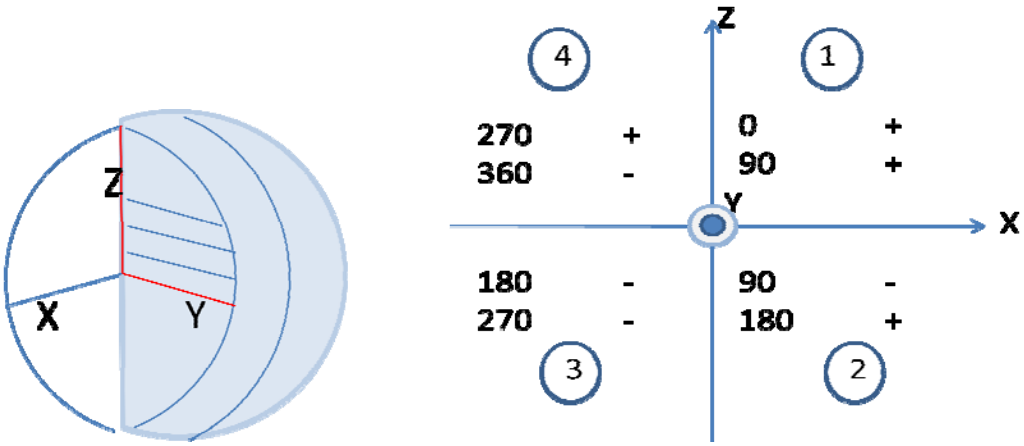

Figure 12: Octants in 3-D space

To simplify understanding this concept a 2-D case is examined here. For example, if the X axis moves to quadrant 1, then the Y axis can only move to quadrants 1 or 2 because by moving X to quadrant 1, the sign of X becomes positive, but since Z is perpendicular to X sign of Z becomes positive too. Therefore, the Y axis can be in either 1st or 2nd quadrants since the value of Z is only positive in these quadrants. During the experiments that were conducted, it was also observed that in the Global method of angle measurement, the order of the movement of the axes is very important. For example, initiating a movement from an octant where X>0, Y>0, and Z<0, if X moves first, then the values of angles are: (360-Θ, Θ, 270- Θ). However, if Y moves first, the angles become: (Θ, 350- Θ, 270- Θ). The tables below show how, due to the lack of one angle of freedom, the calculated values for each octant is repeated in one other octant.

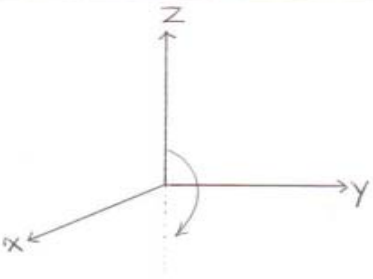

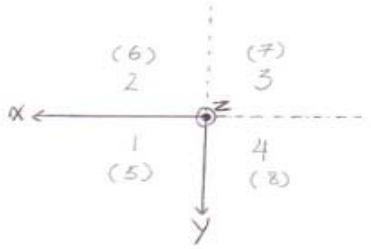

Region 3 : $x > 0$ θ $y > 0$ θ $z > 0$ $360 - \theta$	Region 4 : $x > 0$ θ $y < 0$ $180 - \theta$ $z > 0$ $360 - \theta$
Region 2 : $x < 0$ $180 - \theta$ $y > 0$ θ $z > 0$ θ	Region 1 : $x < 0$ $180 - \theta$ $y < 0$ $180 - \theta$ $z > 0$ θ
Region 7 : $x > 0$ $360 - \theta$ $y > 0$ θ $z < 0$ θ	Region 8 : $x > 0$ $360 - \theta$ $y < 0$ $180 - \theta$ $z < 0$ $270 - \theta$
Region 6 : $x < 0$ $270 - \theta$ $y > 0$ θ $z < 0$ $180 - \theta$	Region 5 : $x < 0$ $180 - \theta$ $y < 0$ $180 - \theta$ $z < 0$ θ

Figure 13: Angle value in different octants

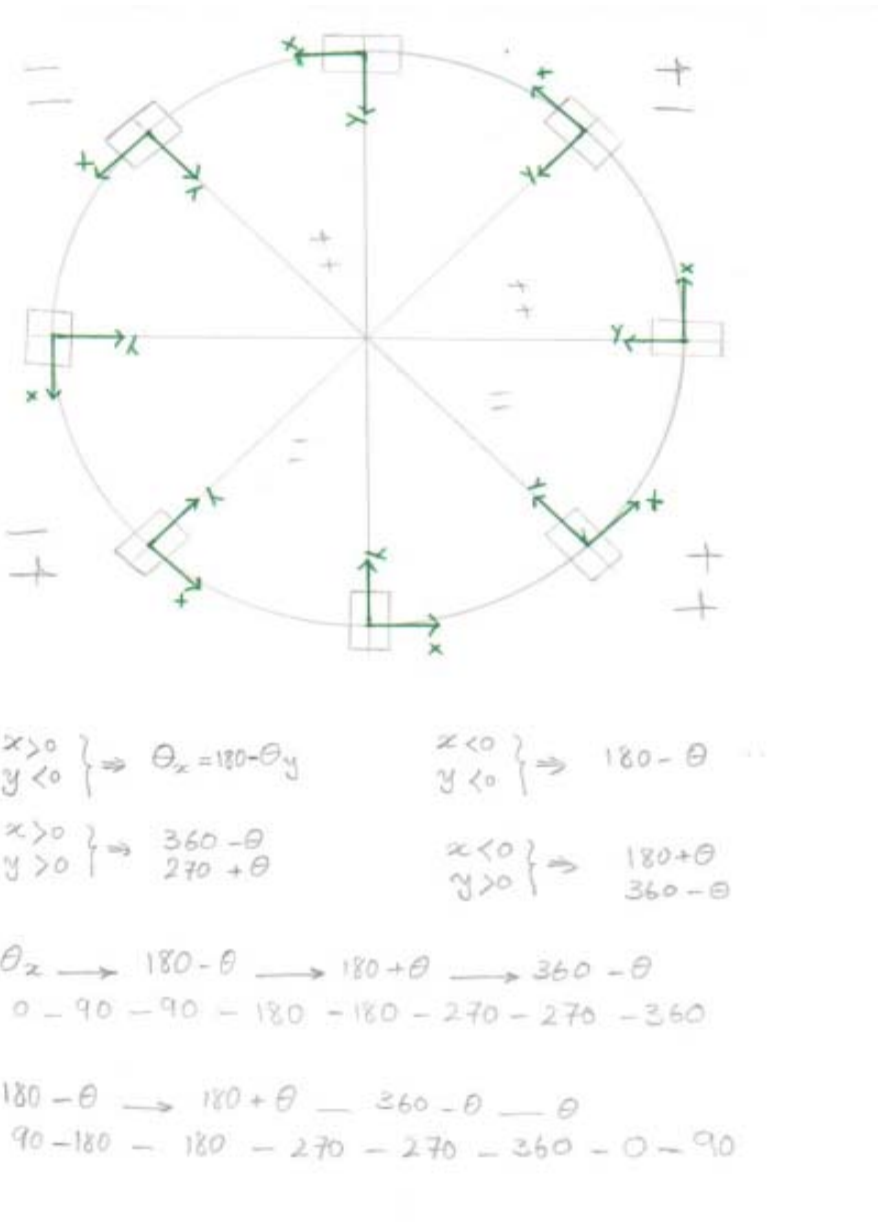

Figure 14: Finding the position of X and Y in the upper or lower octant

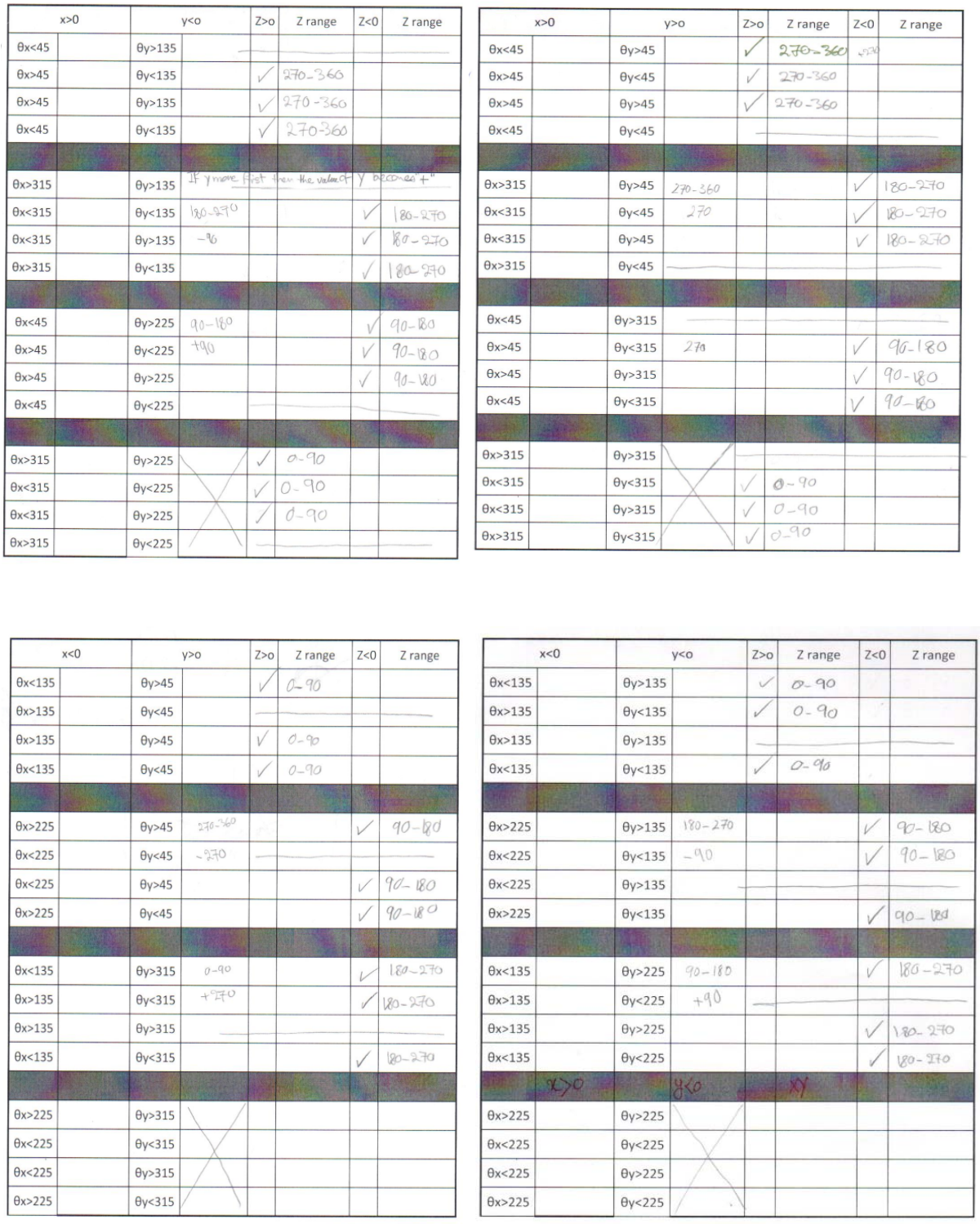

Figure 15: Finding the position of Z according to the position of X and Y

The following three figures illustrate angles that were obtained with respect to gravity from 0° to 360° employing the Global method. It is observed that the angles are repeated. From these

graphs it was concluded that due to the lack of one degree of freedom it is impossible to be able to find angles in the range of 0° to 360° from one accelerometer.

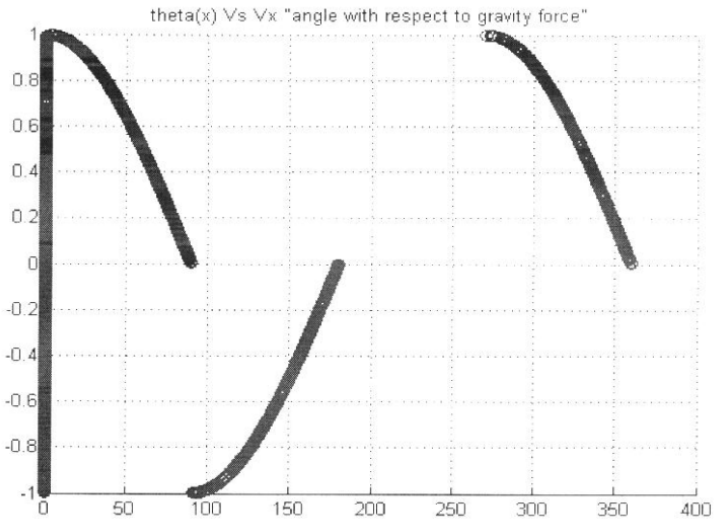

Figure 16: Θ_X versus V_X

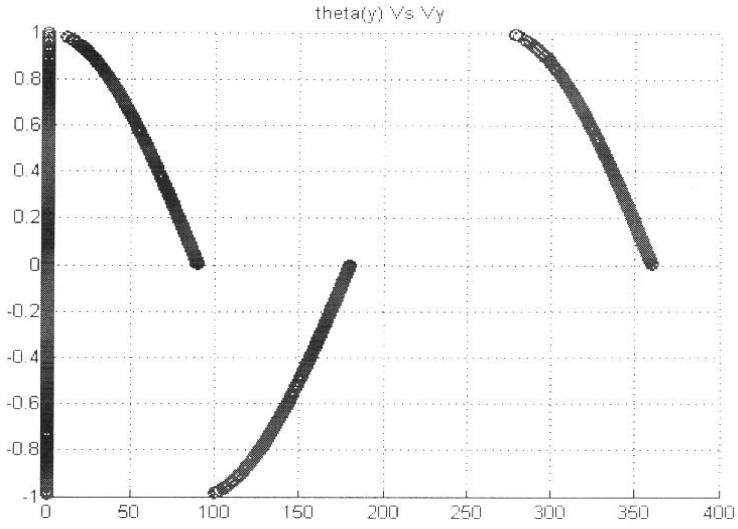

Figure 17: Θ_Y versus V_Y

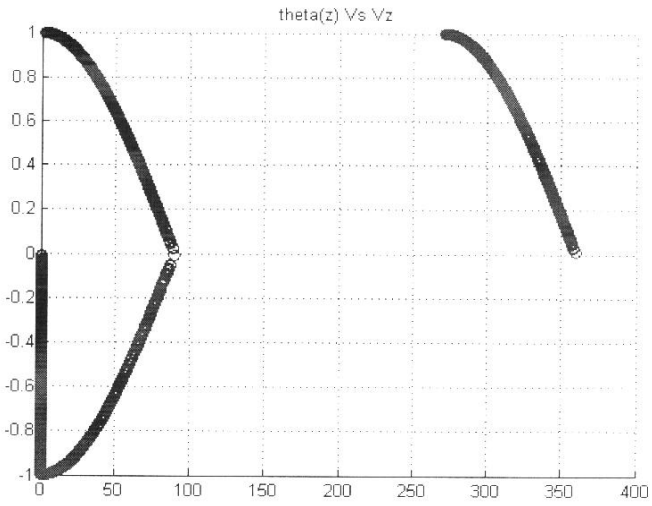

Figure 18: Θ_Z versus V_Z

The angles however, could be measured from -90° to 90° utilizing this method. The following calculations illustrate how the angles could be measured in this case.

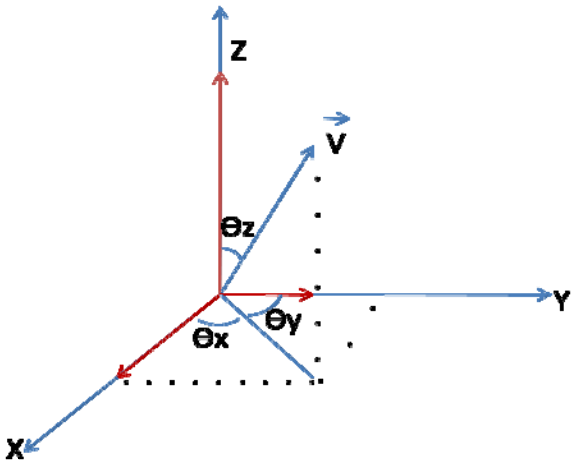

Figure 19: Projection on V onto X, Y, and Z to find the angle of X, Y, and Z

$a.b = a_1 b_1 + a_2 b_2 + a_3 b_3 = |a||b| \cos \Theta$

$a \times b = < a_2 b_3 - a_3 b_2 , a_3 b_1 - a_1 b_3 , a_1 b_2 - a_2 b_1 > = |a||b| \sin\Theta$

To measure the angle of vector V represent measurement of axis of accelerometer in respect to by using the above characteristics.

$\mathbf{V.x} = V_x \rightarrow |\mathbf{V.\ x}| = V_x$

$\mathbf{V} \times \mathbf{x} = < 0, V_z , -V_y >$

$$|\mathbf{V}\times\mathbf{x}| = \sqrt{V_y^2 \quad + \ V_z^2}$$

$$\tan\Theta_x = \frac{|a\times b|}{|a.b|} = \frac{\sqrt{V_y^2 \ + V_z^2}}{V_x}$$

$$\mathbf{V} \cdot \mathbf{y} = V_y \ \rightarrow\ |\mathbf{V}.\ \mathbf{y}| = V_y$$

$$\mathbf{V} \times \mathbf{y} = \langle -V_z\ ,\ 0,\ V_x \rangle$$

$$|\mathbf{V}\times\ \mathbf{y}| = \sqrt{V_x^2 \quad + \ V_z^2}$$

$$\tan\Theta_y = \frac{|a\times b|}{|a.b|} = \frac{\sqrt{V_x^2 \ + V_z^2}}{V_y}$$

$$\mathbf{V.z} = V_z \ \rightarrow\ |\mathbf{V}.\ \mathbf{z}| = V_z$$

$$\mathbf{V} \times \mathbf{z} = \langle V_y\ ,\ -V_x\ ,\ 0 \rangle$$

$$|\mathbf{V}\times\mathbf{z}| = \sqrt{V_x^2 \quad + \ V_y^2}$$

$$\tan\Theta_z = \frac{|a\times b|}{|a.b|} = \frac{\sqrt{V_x^2 \ + V_y^2}}{V_z}$$

Therefore,

$$\begin{bmatrix} A \\ B \\ C \end{bmatrix} = \begin{bmatrix} 0 & \frac{V_Y}{V_X^2} & \frac{V_Z}{V_X^2} \\ \frac{V_X}{V_Y^2} & 0 & \frac{V_Z}{V_Y^2} \\ \frac{V_Y}{V_Z^2} & \frac{V_Y}{V_Z^2} & 0 \end{bmatrix} * \begin{bmatrix} V_X \\ V_Y \\ V_Z \end{bmatrix}$$

$$\begin{bmatrix} \theta_X \\ \theta_Y \\ \theta_Z \end{bmatrix} = \begin{bmatrix} \tan^{-1}\sqrt{A} \\ \tan^{-1}\sqrt{B} \\ \tan^{-1}\sqrt{C} \end{bmatrix}$$

Notes:

Because the output values of the accelerometer are the projection of the gravity acceleration on

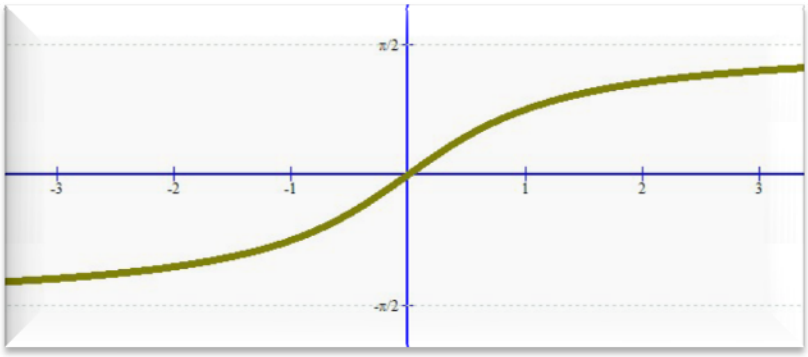

Figure 20: Inverse tangent curve

X, Y , and Z axis the magnitude of their vector addition must be one. For example if Vx = 0.05g, Vy = 0.05g, and Vz = 0.99g then the magnitude of their addition becomes

$$\sqrt[3]{V_x^2 + V_y^2 + V_z^2} = \sqrt[3]{0.05^2 + 0.05^2 + 0.99^2} = 0.995$$

Most of the extracted data don't have the mentioned characteristics which shows that the accelerometers output are not correct.

The Tangent inverse curve approaches infinity which means that the accuracy of calculations increase dramatically after the tangent inverse passes the linear region (between -1 and +1).

The $V = \sqrt[3]{V_x^2 + V_y^2 + V_z^2}$ can be used to make sure that accelerometer's values are correct.

Axis	G Values	Limit G to Maximum 1G	Radians	Degrees	Tangent solution
X	0.11	0.11	1.46057328	83.68468443	83.6611
Y	0.02	0.02	1.55079499	88.854008	88.8497
Z	0.99	0.99	0.14153947	8.109614456	6.4433

V = 0.997 *Acceptable*

Table 1

X	-0.03	-0.03	1.60080083	91.71913132	88.0626
Y	0.11	0.11	1.46057328	83.68468443	82.8791
Z	0.88	0.88	0.49493413	28.35763658	7.3824
		V = 0.923		*Not acceptable*	

Table 2

X	-0.24	-0.24	1.81316218	103.8865404	-71.0986
Y	0.17	0.17	1.39996666	80.21218094	76.7349
Z	0.68	0.68	0.82303369	47.15635696	23.3891
		V = 0.819		*Not acceptable*	

Table 3

So as we see by using the above equation we can check the accuracy of the values before processing them further.

Another problem that was faced in the measurements was that the output signal was a bit distorted. This problem could be overcome by using a digital filter. In the next section more detail on the filter is provided.

- Filter Design

The consequences of using long wires and finite precision equipment with limited sampling frequency are noise and error. Since finite signal resolution and noise destroy signal, signals can be filtered and band limited to provide more desirable results. A digital filter with 5Hz stop-band and 50dB attenuation was designed using the Digital Filter Package in MATLAB. The frequency response of the filter is shown in figure 20. The code of the filter is provided in the appendices. Note that this filter is used in the local approach as well.

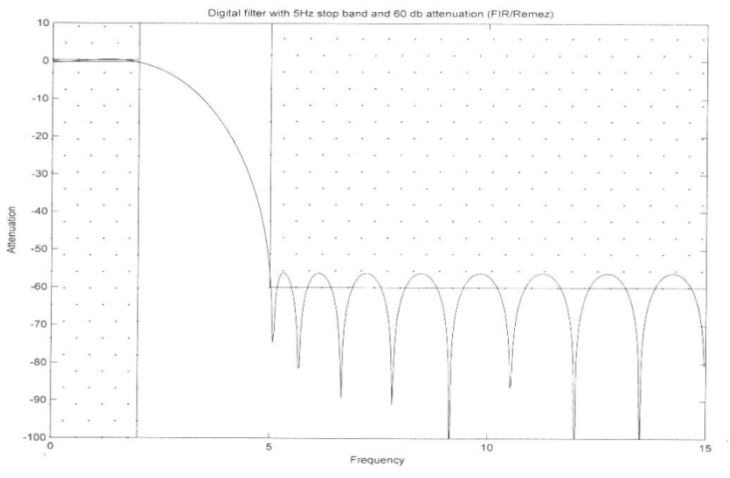

Figure 21: Digital filter with 5Hz stop-band and 50dB attenuation

3. Local measurement

The final and most effective method that was used to measure angles in this project was done base on the local angle measuring principles.

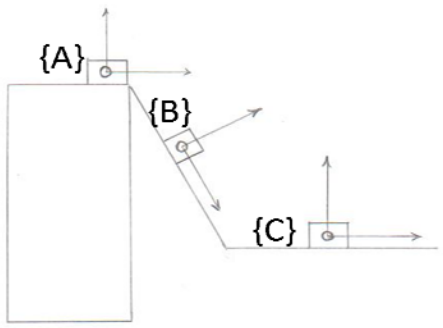

Figure 22: shoulder-bicep and bicep-arm movement

The x, y, and z-axis of the accelerometer mounted on the body is defined as the standard coordinates {A}, and that on the upper limb is defined as the rotational coordinates {B}. In this method the upper limb motion to the body is obtained from the positional relation between {A} and {B}. The rotational transform between these two coordinates is decided with the following notation. The notation is decided that the coordinates {B} agree with the coordinates {A} at the initial states, and rotate ψ angle about the z-axis of coordinates {A} at the first term, rotate φ angle about the y-axis at the next term ,and rotate θ angle about the x-axis at the last term. The matrix of the rotational transform due to this notation is indicated by:

$$R_{zyx} =$$

$$\begin{pmatrix} 1 & 0 & 0 \\ 0 & \cos\phi & -\sin\phi \\ 0 & \sin\phi & \cos\phi \end{pmatrix} \begin{pmatrix} \cos\theta & 0 & -\sin\theta \\ 0 & 1 & 0 \\ \sin\theta & 0 & \cos\theta \end{pmatrix} \begin{pmatrix} \cos\phi & -\sin\phi & 0 \\ \sin\phi & \cos\phi & 0 \\ 0 & 0 & 1 \end{pmatrix}$$

$$= \begin{pmatrix} c\phi c\theta & c\theta s\phi & s\theta \\ x-s\phi s\theta c\phi - s\phi c\phi & -s\theta s\phi s\phi + c\phi c\phi & s\phi c\theta \\ -s\theta c\phi c\phi + s\phi s\phi & -s\phi s\theta c\phi - c\phi s\phi & c\theta c\phi \end{pmatrix}$$

Thus, in this method the component of the gravitation that is acquired after filtering is used. The same filter that was designed for the Global method was used here again. The component of x, y,

z-axis direction in the gravitation loaded on the accelerometer mounted on the body are defined as (g_{x1}, g_{y1}, g_{z1}), and that on the upper limb are defined as (g_{x2}, g_{y2}, g_{z2}). Using the foregoing matrix R_{XYZ}, the relation between (g_{x1}, g_{y1}, g_{z1}) and (g_{x2}, g_{y2}, g_{z2}) is described by the following equation in the same manner as the relation of former acceleration. The ψ, φ, θ were obtained from these two relations.

$$\begin{bmatrix} gx2 \\ gy2 \\ gz2 \end{bmatrix} = R_{zyx} \begin{bmatrix} gx1 \\ gy1 \\ gz1 \end{bmatrix}$$

The raise angle α in up and down directions, and circumflex angle β in forth and back were calculated to express the upper limb motion. To convert the angle ψ, φ, θ into α and β, we described the direction of the z-axis of the accelerometer mounted on upper limb because of the z-axis in direction from the shoulder to the elbow. The direction of the z-axis of {B} for {A} is shown in the next figure using ψ and θ. For this figure, α and β are described by the following equations.

$$\tan\alpha = \frac{\sqrt{\sin^2\psi + \tan^2\theta}}{\cos\theta}$$

$$\tan\beta = \frac{\sin\psi}{\tan\theta}$$

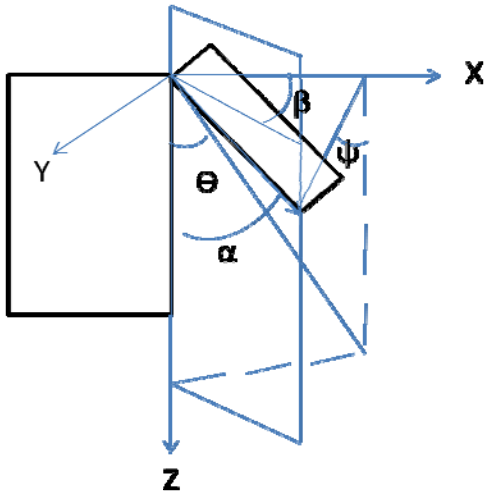

Figure 23: Raise angle and circumflex angle

In the case of one axis joint motion monitoring this method proved to be effective in practice. Therefore this method was acquired to find the shoulder and arm motion. Calculations for finding the angle between arm and bicep are provided below.

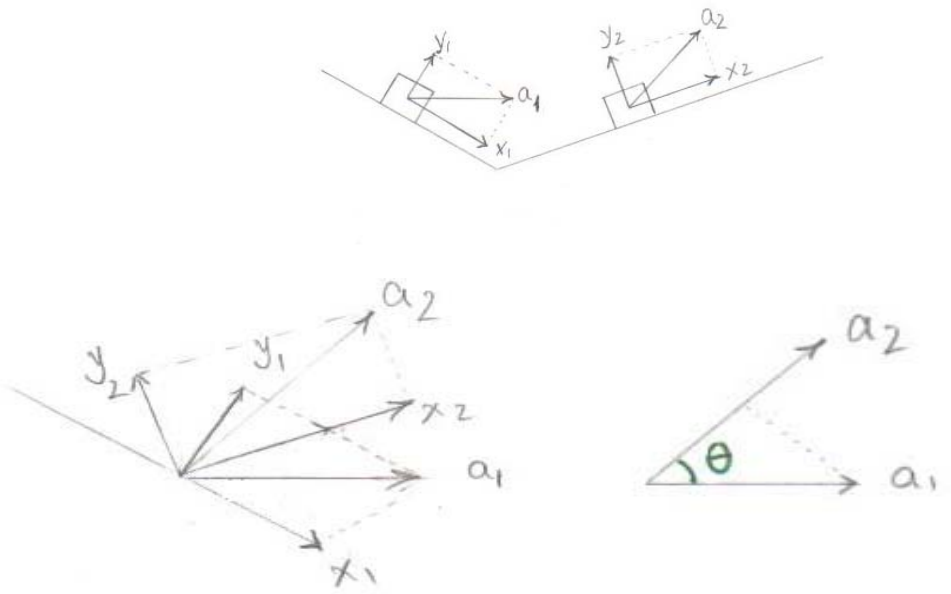

Figure 24: Using two accelerometer to find the angle between joints (such as arm and bicep)

$\mathbf{a_1} . \mathbf{a_2} = x_1x_2 + y_1y_2 + z_1z_2 = |a_1|\ |a_2|\cos\theta$

$\mathbf{a_1} \times \mathbf{a_2} = \langle y_1z_2 - z_1y_2,\ z_1x_2 - x_1z_2,\ x_1y_2 - y_1x_2 \rangle = |a_1|\ |a_2|\sin\theta$

$a_{x1} = a_{x2}\cos\theta - a_{y2}\sin\theta$

$a_{y1} = a_{x2}\sin\theta + a_{y2}\cos\theta$

$x_1 = x_2\cos\theta - y_2\sin\theta$

$y_1 = x_2\sin\theta + y_2\cos\theta$

$$\begin{bmatrix} x1 \\ y1 \end{bmatrix} = \begin{bmatrix} \cos\theta & -sin\theta \\ sin\theta & cos\theta \end{bmatrix} \begin{bmatrix} x2 \\ y2 \end{bmatrix}$$

$\tan\theta = (a_{x2}a_{y1} - a_{x1}a_{y2}) / (a_{x1}a_{x2} - a_{y1}a_{y2})$

- Pseudo inverse method

The pseudo inverse method was tried to find the rotation matrix (R). However, since the matrix R is singular this method was not successful. The way this method works is shown below: assume AR=B, where A and B are not square matrices. Then, matrix R would be equal to:

$$R = (A^T A)^{-1} A^{-1} B$$

3 Design

As mentioned before, next to the problem of human motion emulation, other issues such as the weight of the system, the power supply, and the destructive interference with electromagnetic fields or ferromagnetic materials need to be considered when designing a stand-alone posture and body movement detector. To generate a good design to meet the objectives, the following processes were taken. First, what seemed a feasible design was considered. Second, after conducting more research and gaining more knowledge the design was upgraded and developed more. Finally, after considering the type of input required for each device, the output of different devices, compatibility between the components, size, weight, and cost of different components the finalized design was generated. The design was split into two sections: hardware design and software design. The design consists of a microcontroller that will process data coming from several tri-axis accelerometers. The processed data will get transferred to the serial port of the chip which is connected to a RF module. The data of all sensors is serially transferred from the RF module transmitter to the receiver device connected to a base station. The base station is responsible for any post processing required for cleaning and filtering the incoming data. This step is a crucial element of the design for eliminating undesired data that could halt the system or cause inaccurate movements within the LSM. The data being transferred to the base station for post processing utilizes the COM to communicate between the RF module, the receiver and the base station. In this section of the report detailed description on the approached methods, hardware and software design in this project are provided.

3.1 Approached methods

At first accelerometers were used to detect body motion. However, since accelerometers are not capable of sensing any horizontal movements, in the absence of dynamic range, two solutions were proposed and tested. The first solution was to use compass sensors to be used when a horizontal movement takes place. One of the problems that were faced when implementing this method was that the compass sensor that was used had an active range of $\pm 5°$, meaning that it would detect direction only when placed horizontally having an offset of $+5°$ or $-5°$. This problem was most important for the back motion, because it was of more interest to be able to detect the motion of the back when the body is bent forward and is moved at a constant speed from one side to the other. To tackle this problem, four compass sensors were mounted on a board having 10°angle from each other as shown in the figure below. Therefore, if the person using the device bent for up to 40 degrees, which is quite significant for the back, one of the compasses would be active to detect any horizontal motion taking place after bending. For example, if the person bends for 5 degrees, the first sensor would become on, and if the person bends for 25 degrees, the third compass would become on.

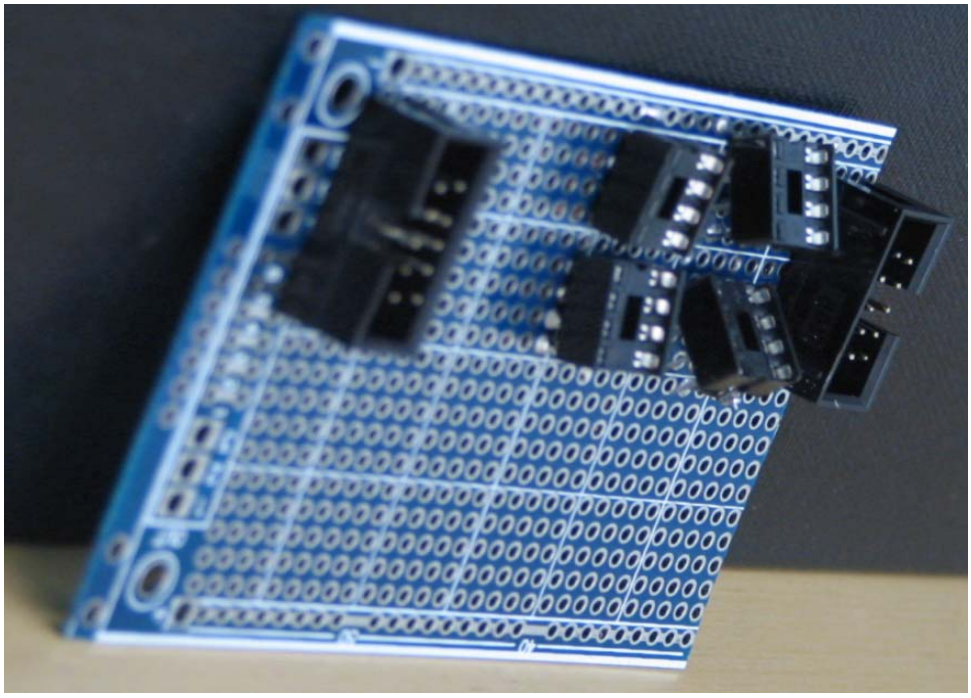

Figure 25: Position of the four compass sensors used for detecting horizontal movement of the back

This method was proven to be effective and used for the final design. Moreover, a gyroscope was also tested. It was observed that the gyroscope along with accelerometers can provide very accurate measurements in human motion emulation. However, due to the high cost of gyroscopes in comparison to compass sensors and time limitations, it was decided to use compass sensors instead of gyroscope.
As mentioned before, for measuring angles using accelerometers, the local method (as explained in section 2.10) was employed. Detailed explanations on the components and the software design are provided in the following sections.

3.2 Hardware Design

The components that were acquired are as the following.

- Sensor: 3D accelerometer and compass
- Microcontroller
- Battery
- RF module

3.2.1 Accelerometer

The sensor that is used in this design is HITACHI H48C tri-axial accelerometer which operates in series. Therefore, there is a chip select to retrieve data from them periodically. What needs to be kept in mind is that the output of the sensors must be measured exactly once for each sensor after one another during sampling. In other words, the microcontroller needs to read data from all sensors periodically without missing or over sampling data from an accelerometer. The way the system was modified to avoid sampling misbehavior was by employing timer and a counter in programming the microcontroller. The sensor has 6 pins which have the following functions:
(1) CLK Synchronous clock input
(2) DIO Bi-directional data to/from host
(3) Vss Power supply ground (0v)
(4) Zero-G "Free-fall" output; active-high
(5) CS Chip select input; active-low

(6) Vdd +5vdc

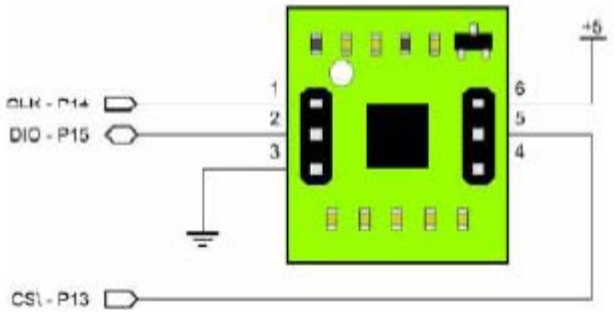

Figure 26: The accelerometer connections

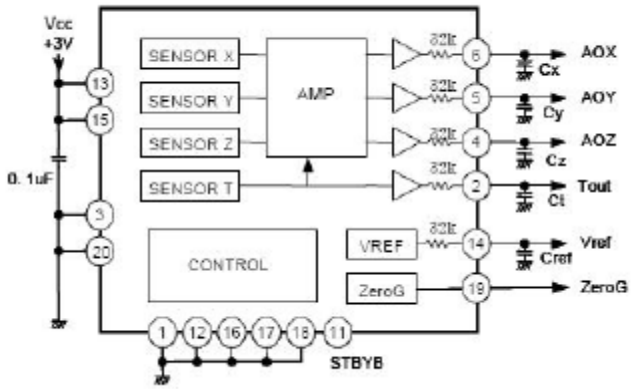

Figure 27: The functional block diagram of the accelerometer

3.2.2 Compass sensor

The compass sensor that was used in this project was the Hitachi HM55B Compass Module. This compass is a dual-axis magnetic field sensor that is sensitive to microtesla variations in magnetic field strength.

3.2.3 Essential Connection

To connect the H48C module to the microcontroller requires just three I/O pins. The CLK and DIO pins are shared in this system due to the use of eight H48C modules. See Figure 2 for

connection details. Through MEMS (Micro Electro-Mechanical System) technology and built-in compensation, the H48C accelerometer provides simultaneous outputs through analog conditioning circuitry to an MCP3204 ADC.

3.2.4 Microcontroller

Basic Stamp 2px microcontroller was chosen for this design. By uniting HI-TACHI H48C MEMS accelerometer with BS2px microcontroller with high number of bits (12)0:2% accuracy can be achieved. Moreover, the accuracy of the system could be increased by using a microcontroller with a higher number of ADC resolution. However, since there would be no point in having a microcontroller with a higher accuracy than the accelerometer it was concluded that BS2px would be sufficient for this design. The only problem with this choice is that the sampling rate of the system with 8 sensors is 8 samples which is more than half of the minimum required sampling rate for a real time system. This problem was overcome by using 2 microcontrollers so that each microcontroller handles 4 sensors instead of 8. Power consumption was another factor that was considered when choosing a suitable microcontroller. Since the whole system must mount on a person, the power consumption must be low so that the system can be used for a long time without adding extra weight to be carried on the person by adding a heavier and therefore stronger power source. In addition the voltage needed to power up the system must be as low as possible while the voltage commonly provided by voltage sources is in the range of 7-15 volts. BS2px microcontroller executes approximately 19,000 PBASIC instructions/sec and includes a built-in voltage comparator (I/O pins P0, P1 and P2) as well as built-in, user-configurable Pull-up Resistor, Schmitt Trigger and Logic Threshold circuitry on every I/O pin.

- Processor Speed = 32 MHz Turbo
- Program Execution Speed = 19,000 instructions/sec.
- RAM Size = 38 Bytes (12 I/O, 26 Variable)
- Scratch Pad RAM = 128 Bytes
- EPROM (Program) Size = 8 x 2K Bytes 4,000 Instructions
- I/O Pins = 16+2 Dedicated Serial

- Voltage Requirements = 5 - 15 Vdc
- Current Draw at 5V = 55 mA Run / 450 A Sleep
- PBASIC Commands = 63
- Size= 1.2"x0.6"x0.4"

Figure 28: Basic Stamp 2px Module

Pin	Name	Description
1	SOUT	Serial Out: connects to PC serial port RX pin (DB9 pin 2 / DB25 pin 3) for programming.
2	SIN	Serial In: connects to PC serial port TX pin (DB9 pin 3 / DB25 pin 2) for programming.
3	ATN	Attention: connects to PC serial port DTR pin (DB9 pin 4 / DB25 pin 20) for programming.
4	VSS	System ground: (same as pin 23), connects to PC serial port GND pin (DB9 pin 5 / DB25 pin 7) for programming.
5-20	P0-P15	General-purpose I/O pins: each can source and sink 30 mA. However, the total of all pins should not exceed 75 mA (source or sink) if using the internal 5-volt regulator. The total per 8-pin groups P0 – P7 or P8 – 15 should not exceed 100 mA (source or sink) if using an external 5-volt regulator.
21	VDD	5-volt DC input/output: if an unregulated voltage is applied to the VIN pin, then this pin will output 5 volts. If no voltage is applied to the VIN pin, then a regulated voltage between 4.5V and 5.5V should be applied to this pin.
22	RES	Reset input/output: goes low when power supply is less than approximately 4.2 volts, causing the BASIC Stamp to reset. Can be driven low to force a reset. This pin is internally pulled high and may be left disconnected if not needed. Do not drive high.
23	VSS	System ground: (same as pin 4) connects to power supply's ground (GND) terminal.
24	VIN	Unregulated power in: accepts 5.5 - 12 VDC (7.5 recommended), which is then internally regulated to 5 volts. Must be left unconnected if 5 volts is applied to the VDD (+5V) pin.

Figure 29: Basic Stamp 2px Pin Description

3.2.5 Battery

The battery chosen for this project is Acer BTP-44A3. The voltage current needed for each component in the design are provided in table 4. Note: The microcontroller does not need any voltage regulator because it has internal regulator. However, since the op-amps use battery as the power source, it is better to use regulator to be sure that the op-amp works properly without any loss in the power supply voltage.

#	Component name	Voltage	Current	Source
1	Micro controller 386 Microcontroller 586	12 V 24	160 mA 110	14.8V/6600 mAh 2 of above source
2	Sensors	3.3 V	14 mA	Microcontroller
3	Communication device	3.3 V	x	Microcontroller
4	Relay op-amp [5]	7 V	14 mA	7.4V / 800 mAh

Table 4: Voltage and current required for each component

3.2.6 Communication Interface

For wireless communication an RF module was used. The chosen module was the XBee multipoint RF module since it has low-cost and is easy to deploy. The transmitter and the receiver can be easily connected to the microcontroller board and the computer, respectively, with a USB connector.

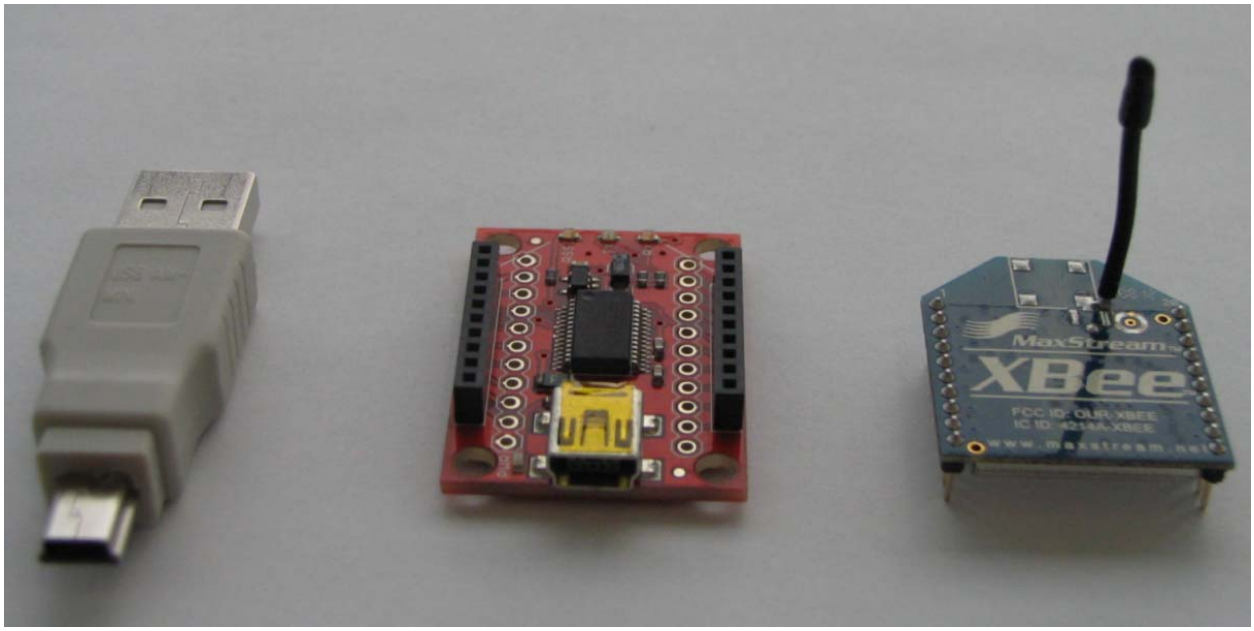

Figure 30: The transmitter, receiver, and the USB connector

- Power output:
  - 2mW (+3 dBm) boost mode
  - 1.25 mW (+1 dBm) normal mode
- Indoor/Urban range: Up to 133 ft (40 m)
- Outdoor/RF line-of-sight range: Up to 400 ft (120 m)
- RF data rate: 250 Kbps

- Interface data rate: Up to 1 Mbps software selectable
- Operating frequency: 2.4 GHz
- Receiver sensitivity:
    - -96 dBm boost mode
    - -95 dBm normal mode

3.3 Software Design

As mentioned in the previous sections connecting the HITACHI accelerometer or the compass sensor to the microcontroller 3 I/O pins requires:

- chip select(CS)
- clock (CLK)
- digital input output (DIO)

1. The clock synchronizes the microcontroller with the accelerometer
2. The CS connects and disconnects a specific accelerometer to/ from the microcontrollers
3. DIO is a bi-directional input/output pin

3.3.1 Software Algorithm

One of the first concerns before software design was to make sure the PC and the microcontroller I/O ware synchronized. In other words the order of choosing a sensor when reading data was to be synchronized with the order of linking the captured data to the LSM. Four pins of each microcontroller (P4, P5, P6, and P7) are used as the chip select of accelerometer. Each accelerometer becomes on when the corresponding chip select is high. Then, the gravitational and dynamic acceleration sensed by each axis of rotation is sent serially to the microcontrollers ADC. Right after turning the chip select high, the microcontroller starts the timer and the counter. The timer is used to make sure that non of the accelerometers stays on more than 16.6 ms [each microcontroller handles 4 accelerometer and for a real time system at least 15 samples are needed. Therefore, 1/ 15×4 = 0:01667s.]

The counter as a safety valve to make sure that not more than one set of samples (one sample per axis) is captured. The ADC reads the data and converts it to a number in the range of 1400 to

1600. Next, the angle is calculated by using the $\tan^{-1}$ function. For the purpose of our calculation the value between $\pm$ 1g is needed. Therefore, a limiter is used to limit the value of the input of the AD to $\pm$ 1g. Due to the presence of the dynamic acceleration, a fast motion in the positive g direction adds to the gravitational acceleration and vice versa. As a result a software limiter is implemented in the code to limit the change between two consecutive samples to specific angle. In other words, if the difference between the two angles is more than the accepted range, the value of the erroneous angle will be replaced by the previous angle value. The reason for performing the calculations in the computer and not on the microcontroller is that, the $\tan^{-1}$ or any other trigonometric functions were not supported on the microcontroller. Therefore, to find $\tan\theta$, the easiest way would be to find sine and cosine by using their series representation, and then divide sine by cosine to get the tan function. Then, the series had to be implemented on the microcontroller. This method would take much longer to calculate the angles than performing the calculations on the computer. The series representation of sine and cosine are provided in the appendix. The calculated data at this point is sent to the base station via either RF module or USB cable. The data received in the base station, which is in the form of Euler angles, is converted to unit quaternion for further calculations in the LSM.

4 Discussion and Conclusion

Stand-alone motion emulation devices that exist in the market usually have prices in the range of thousands of dollars, because next to the complex software design, most of these devices use gyroscopes as well as other sensors. The objective of this project was to not only detect human motion, but also make the device as low costly as possible. The task of detecting motion in a 2-D space was accomplished. However, to detect motion in 3-D space using accelerometers, accelerometers should be used in a local system. In other words, by obtaining the angles that accelerometers provide with respect to gravity, 3-D motions cannot be detected. However, if for example, accelerometers are connected on both sides of a joint (let's say arm and bicep), it is possible to find the angle between accelerometers as the arm moves. Hence, the changes in the joint angle can be emulated. However, the complexity of the calculations is significant; any movement in the 3-D space can be defined base on pitch, roll, and yaw rotations. Therefore,

when an object moves from point A to B (in 3-D space), by having the coordinates of A, the order of rotations (for example, whether it was roll, pitch, yaw or yaw, roll, pitch, …) and the rotational angle, the coordinates of B can be found easily by using the rotation matrices. However, solving for the angular rotations based on coordinates of A and B is very complex, because many different rotations can take an object in 3-D space from A to B. Moreover, since the obtained data from the coordinate axes are dependant on each other, as explained before, pseudo-inverse method in solving for the rotation matrix would not work since the rotational matrix R is singular. A lot of time was spent on studying this problem and finding a solution for it. Unfortunately, non of the taken approaches was successful. It is highly recommended to study rotations in 3-D space in more depth for future work. Also, another approach that could perfectly work and is equally suggested would be the use of gyroscope when the cost does not introduce any constraints. In conclusion, the project was worthwhile and was accomplished to a great and satisfactory extend.

6 Block Diagram

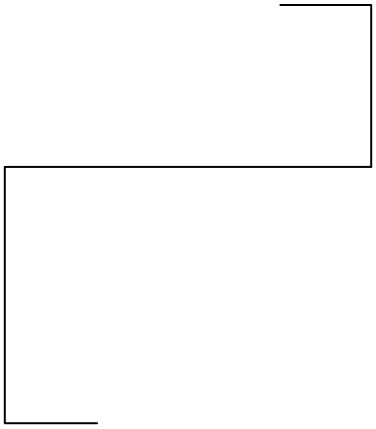

7 References

[1] Abdoli-Eramaki M., Stevenson JM., Agnew MJ., Kamalzadeh A. 2007. "Comparison of 3D dynamic virtual model to link segment model for estimation of net L4/L5 reaction moments during lifting."

[2] Sciavicco L, Siciliano B. "Modeling and Control of Robot Manipulators."

[3] http://www.alldatasheet.com/datasheet-pdf/pdf/186278/ETC/DE-ACCM3D.html

[5]Texas Instrument, [*www.ti.com*]

[6] http://www.alldatasheet.com/datasheet-pdf/pdf/53577/FAIRCHILD/LM317T.html

[7] http://en.wikipedia.org/wiki/Euler_angles

[8] http://en.wikipedia.org/wiki/Gimbal_lock

[9] http://en.wikipedia.org/wiki/Conversion_between_quaternions_and_Euler_angles

[10]

[http://www.westcoastpower.org/acer2311657.html?gclid=COKnroLVlJcCFQMnGgod2kyP_A]

[11] http://www.global-battery.co.uk/camcorder-batteries/jvc-gr-d270u.htm

[12] http://www.digi.com/products/wireless/zigbee-mesh/xbee-zb-modulespecs.jsp

[13] http://www.digi.com/pdf/ds_xbeemultipointmodules.pdf

8 Appendix

The series representation of sine and cosine:

$$\sin x = x - \frac{x^3}{3!} + \frac{x^5}{5!} - \frac{x^7}{7!} + \cdots$$

$$= \sum_{n=0}^{\infty} \frac{(-1)^n x^{2n+1}}{(2n+1)!} = \sum_{\text{odd } m \geq 1} (-1)^{(m-1)/2} \frac{x^m}{m!},$$

$$\cos x = 1 - \frac{x^2}{2!} + \frac{x^4}{4!} - \frac{x^6}{6!} + \cdots$$

$$= \sum_{n=0}^{\infty} \frac{(-1)^n x^{2n}}{(2n)!} = \sum_{\text{even } m \geq 0} (-1)^{m/2} \frac{x^m}{m!}.$$